Journal of Physics: Conference Series

PAPER • **OPEN ACCESS**

Synthesis of $REBa_2Cu_3O_{7-\partial}$ (RE=Nd, Eu, Gd) Nanoparticles by Wet-Mixing Method

To cite this article: W.G. Suharta *et al* 2018 *J. Phys.: Conf. Ser.* **1091** 012027

IOP Conf. Series: Journal of Physics: Conf. Series **1091** (2018) 012027 doi:10.1088/1742-6596/1091/1/012027

Synthesis of $REBa_2Cu_3O_{7-\partial}$ (RE=Nd, Eu, Gd) Nanoparticles by Wet-Mixing Method

W.G. Suharta[1], P. Suardana[1], Windaryoto[1], S. Pratapa[2], S. Suasmoro[2], D. Darminto[2], Y. Ishii[3], W. Isao[3]

[1] Department of Physics, Faculty of Mathematics and Natural Sciences, Udayana University

[2] Department of Physics, Faculty of Mathematics and Natural Sciences, Institutes of Technology Sepuluh Nopember, Kampus ITS Sukolilo, Surabaya 60111, Indonesia

[3] Advanced MESON Science, Laboratory, RIKEN, 2-1 Hirosawa, Wako, Saitama, 351-0198, Japan

E-mail: wgsuharta@gmail.com

Abstract. The $Nd_{0.33}Eu_{0.33}Gd_{0.33}Ba_2Cu_3O_{7-\partial}$ (NEG-123) nanoparticles have been successfully synthesized by wet-mixing method using HNO_3 as dissolving agent. The NEG-123 samples are divided into two which were treated differently. The first and second samples were mixed respectively, for one and 24 hours. All the samples were then calcined at 600°C for 3 hours, and sintered at relatively low temperature (750 to 900°C), each for 30 minutes. Samples were characterized using X-ray diffraction (XRD), transmission electron microscopy (TEM), and vibrating sample magnetometer (VSM). Rietveld analysis shows the lattice parameter of *a*-axis decreases with the increasing sintering temperature from 750 to 900°C, while the lattice parameter of *b* and *c*-axes increases. Further, it was known based on the XRD analysis that the higher the sintering temperature, the greater the peak intensities and average crystal size. The NEG-123 samples with the average crystal size of hundreds nanometer exhibit paramagnetism, while those with average crystal size of ten nanometers demonstrate superparamagnetism at room temperature.

Keywords : nanoparticle; wet-mixing method; paramagnetism; superparamagnetism

1. Introduction

Since the discovery high-temperature ferromagnetism that reported in alkaline-earth hexaboride, research about nano-particle more intensively conducted in several countries. Practically, magnetic nano-particle used as active components of ferrofluids, in recording tapes, and in biomedical applications [1, 2].

Ferromagnetism properties at room temperature in nano-particle of non-magnetic and magnetic oxides such as CeO_2, TiO_2, MgO and Al_2O_3 have been widely studied. The origin of ferromagnetism in these nano-particle suggested due to magnetic moments arising from oxygen vacancies at the surfaces of the nanoparticle, as has been reported by Sundaresan et.al [3]. Ghosh et.al has synthesized zinc sulphide nano-particles to be used as devices of field emission [4]. Also, oxygen vacancies at the surfaces of the nanoparticle has been studied by Gang Niu et.al, on Pr doped CeO_2 [5].

Research on nanoparticle has not been only limited to the synthesis of composite materials, but also on superconductors. In the case of superconducting materials, the $Ba_2Cu_3O_{7-\delta}$ (YBCO, Tc = 91 K)

nanoparticle was firstly reported to exhibit ferromagnetism at room temperature, while its YBCO crystalline bulk, obtained by heating the nanoparticle at 940°C, showed a linear magnetization curve. Across the superconducting transition temperature, the magnetization curve changes from that of a soft ferromagnetic to a superconductor, as has been reported by Shipra et.al [6]. Ferromagnetism in 2212 phases of Bi-Sr-Ca-Cu-O nano-superconductors were also obtained by Baqiya et.al [7]. Furthermore, M. Muralidhar et.al [8] fabricated nano-structured high Tc superconductor of NEG-123 with 30 mol % Gd-211 for application in medicine. V.S. Vinila et.al has also done research on making ceramic nanocrystalline superconductor of GBCO at variation of temperature [9].

In this study, we fabricated nano-particles of $Nd_{0.33}Eu_{0.33}Gd_{0.33}Ba_2Cu_3O_{7-\delta}$ (NEG-123) by wet-mixing method. In this case, the Y element on the YBCO superconductor is replaced by the rare earth element. Substitution and replacement of the Y element with the rare earth element in YBCO superconductor have been done by many researchers, such as by Suharta et.al. He has succeeded in synthesizing RE-123 superconductor with variations of RE elements [10]. Addition or replacement element with the rare earth element is not only done on the YBCO superconductor, but also done on the BSCCO superconductor, as has been done by Suharta et.al [11].

2. Experimental Method

$Nd_{0.33}Eu_{0.33}Gd_{0.33}Ba_2Cu_3O_{7-\delta}$ samples were prepared by wet-mixing method with HNO_3 as dissolving agent. Powders of Nd_2O_3, (99,9 %), Eu_2O_3 (99,9 %), Gd_2O_3 (99,9 %), $BaCO_3$ (99,9 %), and CuO (99,9 %) were used as starting materials. Synthesis process was as follows : the first, the raw material of Nd-123 was mixed and stirred in HNO_3 for 30 minutes, calcined at 600°C for 3 hours and sintered with various temperature (750-900°C), each for 30 minutes. The second, the raw materials of NEG-123 were mixed and stirred in HNO_3 for 24 hours, calcined at 600°C for 3 hours and sintered with variations of temperature (750-900°C), each for 30 minutes. The structure of the samples was examined using X-ray diffraction (Cu*Kα* radiation, 10-90° 2θ-range with a step size of 0,02°). Rietveld refinements to acquire the crystal data of phases for each synthesized material performed using Rietica software by employing Thompson-Cox-Hasting pseudo-Voigt peak shape function. TEM images of the samples were collected to investigate the morphology and distribution of the grains and determine their size. The magnetic hysteresis was measured using a vibrating sample magnetization (VSM Oxford 1,2 T).

3. Results and Discussion

The XRD patterns of the NEG-123 samples prepared by mixing for 30 minutes and sintering at varying temperature for 30 minutes are shown in Fig. 1. While those with mixing for 24 hours and sintering with various temperature for 30 minutes are given in Fig. 2. In general, the diffraction pattern shows sharp peaks, indicating that the crystalline phase has grown well with dominant NEG-123 phase having orthorhombic structure. The $BaCO_3$, $BaNd_2O_4$, $BaCuO_2$, Nd_2BaCuO_5 compounds as minor impurities observed at around 27-32°. The additional sintering temperature has been performed to eliminate impurities and to achieve a single NEG-123 phase. It can also be seen in Fig. 1 and 2 (insert) demonstrating the degradation of $BaCO_3$ compound. A further additional sintering temperature from 750 to 900°C has increased the volume fraction of the NEG-123 phase from 84.3 to 95.9 %.

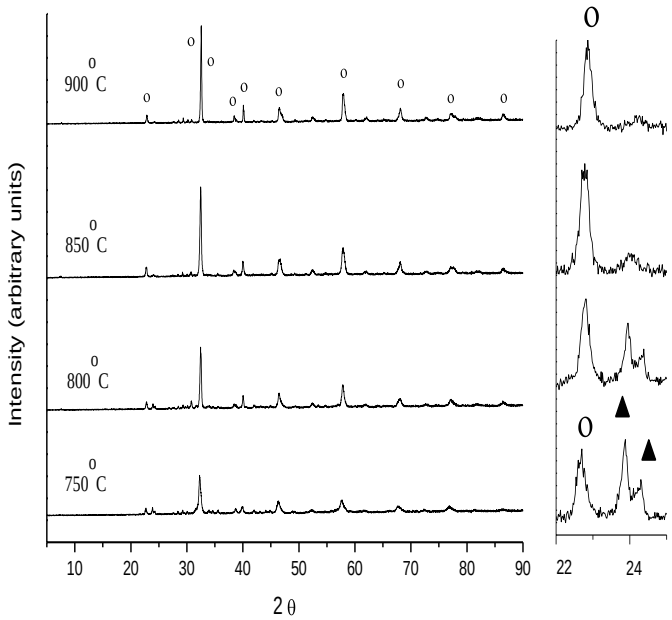

Figure 1. XRD patterns (Cu*Kα* radiation) of the NEG-123 samples prepared with mixing for 30 minutes and sintering for 30 minutes. Insert : NEG-123 samples at 2θ=23-31°.
Symbol :○ NEG-123, ▲ $BaCO_3$

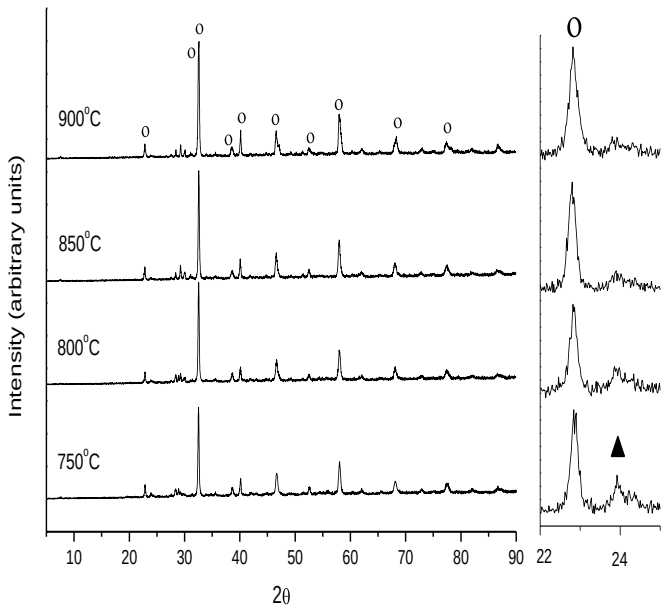

Figure 2. XRD patterns (Cu*Kα* radiation) of the NEG-123 samples prepared with mixing for 24 hours and sintering for 30 minutes. Insert : NEG-123 samples at 2θ=23-31°.
Symbol :○ NEG-123, ▲ $BaCO_3$

The Rietveld analysis on the XRD data in Fig. 1 has produced lattice parameter values (a, b, c) for each sample as shown in Fig. 3(a) for NEG-123 samples. The curve shows the lattice parameter of *a* decreasing with the additional sintering temperature, while *b* and *c* increases. The value of *a* is smaller than that of *b* on sintering temperature below 800°C. It would be resulting negative values of orthorhombic strain. The *a* is greater than *b* on sintering temperature above 800°C, producing positive orthorhombic strain. Furthermore, Fig. 3(b) shows the value of the lattice parameter of NEG-123 samples analyzed from data in Fig. 2. The results are consistent with the former group of NEG-123 samples, where the lattice parameter of *b* and *c* increases with additional sintering temperatures, while *a* decreases.

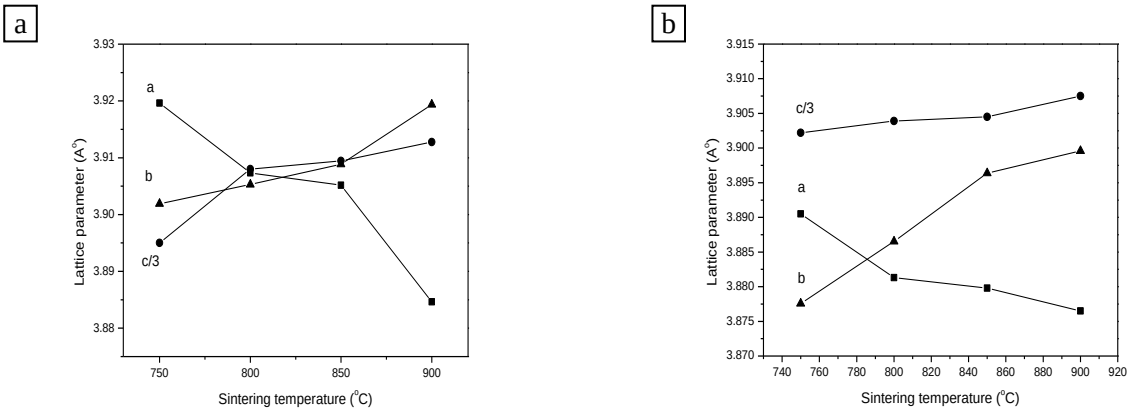

Figure 3. The lattice parameter of NEG-123 samples prepared with various sintering temperature (from 750 to 900°C) and mixing for (a) 30 minutes, and (b) 24 hours.

The solid particle size of the crystal can be determined using Scherrer equation and Rietica software. The effect of sintering temperature on the mean particle size for NEG-123 samples that has been mixed for 30 minutes and sintered for 30 minutes showed the average particle size was greater than 150 nm (Fig. 4a). This indicates that the sintering temperature increasing from 750 to 900°C has already led to agglomeration. So, it can said that is, the higher the sintering temperature, the greater the average crystal size. Similar to the results of the first sample, the average particle size of the second sample increases with increasing sintering temperature, as shown in Fig. 4(b).

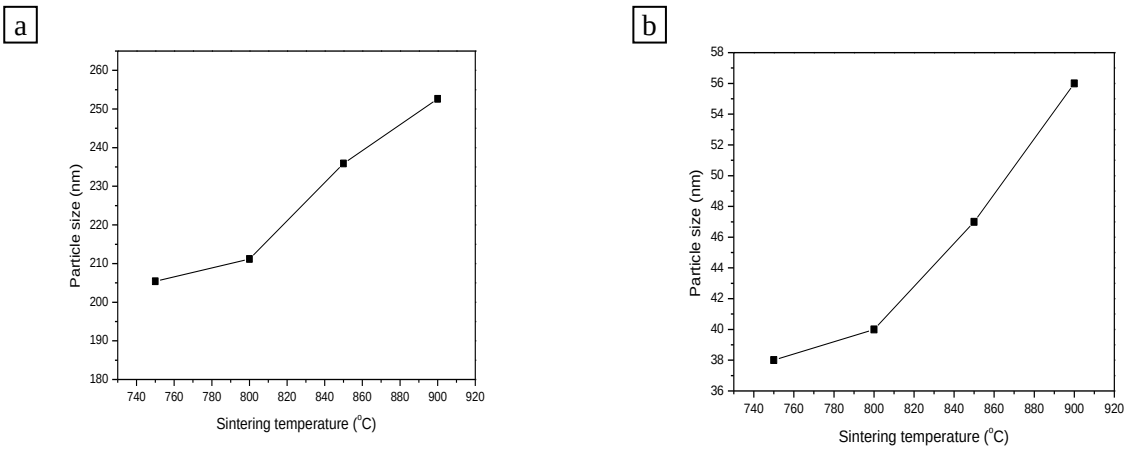

Figure 4. Particle size with increasing sintering temperature of the NEG-123 samples prepared using a set of mixing/sintering time : (a) 30 minutes/30 minutes, (b) 24 hours/30 minutes.

TEM morphology of NEG-123 samples that mixed for 30 minutes and sintered at a temperature of 750, 800 and 900°C for 30 minutes showed in Fig. 5. It showed the particle size of the sample with a sintering temperature of 750 and 800°C in a scale of 100 nm, while the particle size of the sample with sintering temperature of 900°C in the scale of 500 nm. In general shape of NEG-123 particles at a temperature of the 750-900°C showed rod-shape.

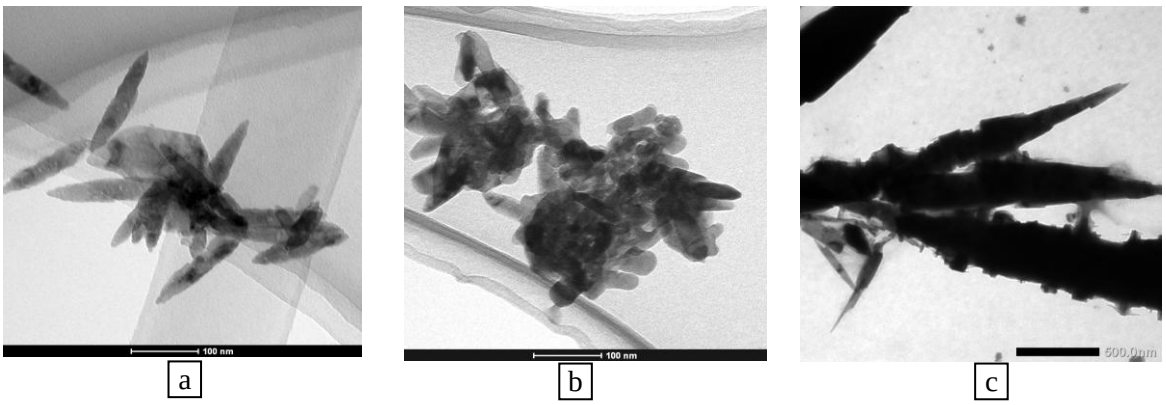

Figure 5. TEM images of NEG-123 samples which were mixed for 30 minutes and sintered for 1 hour at : (a) 750°C, (b) 800°C, (c) 900°C

The morphology of NEG-123 samples that mixed for 24 hours and sintered at 750, 800 and 900°C for 30 minutes observed using TEM are shown in Fig. 6. The morphology is seen to be more homogeneous distribution of particles with average particle size between 20-30 nm as shown in Fig. 6(a) and Fig. 6(b). Meanwhile, the sample that was sintered at 900°C has a bigger average particle size between 20-250 nm and shows a less homogeneous distribution, indicating that agglomeration has already begun because of sintering as shown in Fig. 6(c). In general shape of NEG-123 particles at a temperature of 750-900°C showed spherical-shaped.

The difference in treatment resulted in differences in the shape and size of the particles. There are two possibilities, the first, because longer mixing produces the ionic bond. The second, because of the agglomeration process, in which a short time sintering produces crystal size smaller than a longer sintering time.

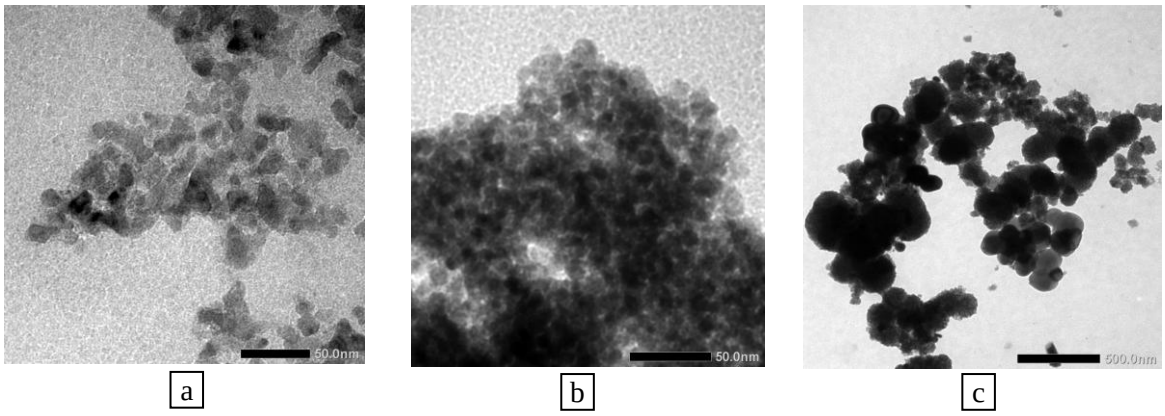

Figure 6. TEM images of NEG-123 samples that were mixed for 24 hours and sintered for 30 minutes at : 750°C, (b) 800°C and (c) 900°C

Going further to the magnetic properties of NEG-123 samples, measured using VSM at room temperature. The NEG-123 samples that mixed for 30 minutes and sintered at 750, 800 and 900°C did not show any hysteresis, but only exhibited paramagnetic properties as shown in Fig. 7(a). Contrarily, for the samples that mixed for 24 hours and sintered at 800, 850, 900°C and 750°C (insert) showed a superparamagnetic properties at room temperature, as show in Fig. 7(b). This effect may probably come from the oxygen vacancies on the sample surface because of having a much larger surface area in the lowering particle size, as suggested previously.

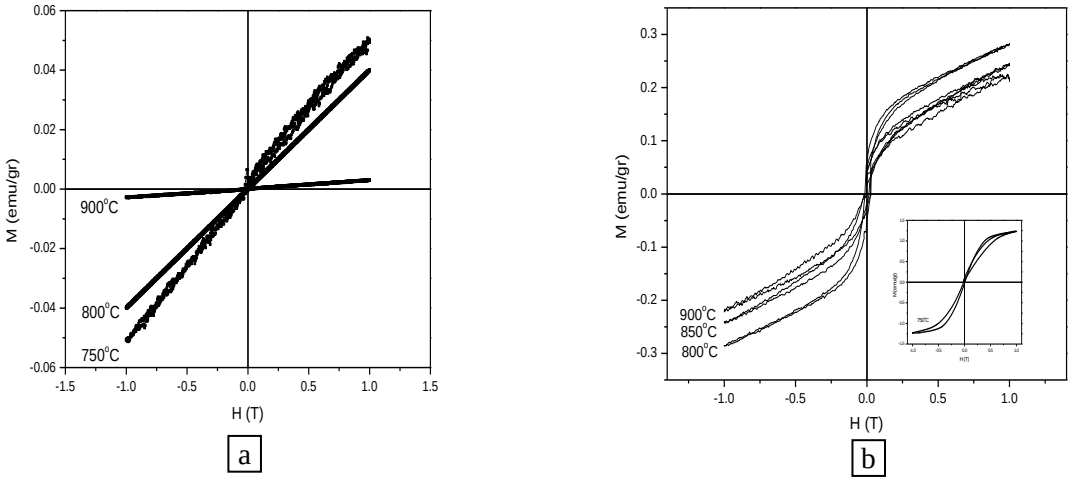

Figure 7. VSM images of (a) NEG-123 samples mixed for 30 minutes and sintered at 750, 800 and 900°C for 30 minutes, (b) NEG-123 samples mixed for 24 hours and sintered at 750, 800, 850 and 900°C for 30 minutes

The magnetization curve showed that the addition of the sintering temperature of 750°C to 900°C resulted in the value of the saturation magnetization (M_S) gets smaller. These results are consistent with the results of TEM characterization, where the addition of the sintering temperature causes the particle size increases and then result in coercive and saturation decreases because the particles form a multidomain. Similar results were obtained by Sundaresan et al., in which the magnetic moment saturation of nano particles is reduced by the addition of particle size.

The nanoparticles have a large surface area, whereas the formation of the surface energy, lower than in the samples in bulk. Low energy on nano particles cause defects on the surface in an amount sufficient. The magnetization can explained by the presence of magnetic cluster which has superparamagnetic properties. However, the sintering temperature increase resulted the larger of energy, so that the particle size increases and the concentration of defects decreases and then magnetic properties disappear.

Conclusions

The NEG-123 nanocrystals have successfully been synthesized by using wet-mixing method. The introduction of additional sintering temperature from 750°C to 900°C can improve the crystallization of the sample marked with the made-up diffraction peak intensity. The increasing sintering temperature has led to the decreasing lattice parameter of a-axis, as well as increasing the lattice parameter of b and c-axis. And then, the higher of sintering temperature, the greater of average crystal size. NEG-123 samples with average crystal size of hundreds nano-scale showed paramagnetic

properties, while NEG-123 with the average crystal size of tens of nano-scale showed superparamagnetic properties at room temperature.

References

[1] Akbarzadeh A, Samiei M and Davaran S 2012 *Nanoscale Res Lett* **7 1** 144.
[2] Issa B, Obaidat I M, Albiss B A and Haik Y 2013 *Int. J. Mol. Sci*. **14 11** 21266-21305.
[3] Sundaresan, Bhargavi R, Rangarajan N, Siddesh U, Rao CNR 2007 *Phys. Rev. B* **74** 161306.
[4] Ghosh S C, Thanachayanont C and Dutta J 2014 *The 1st ECTI Annual Conference (ECTI-CON2004) Pattaya* 145-148.
[5] Niu G, Hildebrandt E, Schubert M A, Boscherini F, Zoellner M H, Alff L, Walczyk D, Zaumseil P, Costina I, Wilkens H and Schroeder T 2014 *ACS Appl. Mater. Interfaces* **6 20** 17496-17505.
[6] Shipra, Gomathi A, Sundaresan A, Rao CNR 2007 *Solid State Communications* **142** 685-688.
[7] Baqiya M A, Widodo H, Rochmawati L, Darminto, Adachi T and Koike Y 2012 *AIP Conf. Proc*. **1454** 260.
[8] Muralidhar M, Koblischka MR and Tomita M 2012 *Current Microscopy Contrbution to Advances in Science and Technology* 1468-1479.
[9] Vinila V S, Jacob R, Mony A, Nair H G, Issac S, Rajan S, Nair A S, Satheesh D J, Isac J 2014 *Journal of Crystallization Process and Technology* **4** 168-176
[10] Suharta W G, Suasmoro S, Pratapa S, Darminto 2013 *AIP Conference Proceedings* **1555** 62-66.
[11] Suharta W G, Widagda I G A, Putra K, Suyanto H 2016 *Journal of Physics: Conference Series* 012006.